bioRxiv preprint doi: https://doi.org/10.1101/146159; this version posted June 5, 2017. The copyright holder for this preprint (which was not certified by peer review) is the author/funder. All rights reserved. No reuse allowed without permission.

The collective influence of 1, 25-dihydroxyvitamin D_3 with physiological fluid shear stress on osteoblasts

Yan Li[1,2,*], Jiafeng Yuan, Qianwen Wang[1,2], Lijie Sun[1,2], Yunying Sha[1,2], Yanxiang Li[1,2], Lizhong Wang[1,2], Zhonghua Wang[1,2]

[1] School of Pharmacy, Taizhou polytechnic college, Taizhou 225300, China

[2] Bone Tissue Engineering Research Center of Taizhou, Taizhou 225300, China

*Corresponding author. Address: School of Pharmacy, Taizhou polytechnic college, Taizhou 225300, China. Fax: +86 523 86664037.

E-mail address: 55397507@qq.com (Yan Li).

bioRxiv preprint doi: https://doi.org/10.1101/146159; this version posted June 5, 2017. The copyright holder for this preprint (which was not certified by peer review) is the author/funder. All rights reserved. No reuse allowed without permission.

Abstract

1, 25-dihydroxyvitamin D_3 (1, 25 $(OH)_2$ D_3) and mechanical stimuli in physiological environment play an important role in the pathogenesis of osteoporosis. The effects of 1, 25-dihydroxyvitamin D_3 alone and mechanical stimuli alone on osteoblasts have been widely investigated. This study reports the collective influences of 1, 25-dihydroxyvitamin D_3 and flow shear stress (FSS) on biological functions of osteoblasts. 1, 25 $(OH)_2$ D_3 were constructed in various kinds of concentration (0, 1, 10, 100 nmmol/L), while physiological fluid shear stress (12 dynes/cm^2) were produced by using a parallel-plate fluid flow system. 1, 25 $(OH)_2$ D_3 affects the responses of ROBs to FSS, including the inhibition of NO releases and cell proliferation as well as the promotion of PGE_2 releases and cell differentiation. These findings provide a possible mechanism by which 1, 25$(OH)_2$ D_3 influences osteoblasts responses to FSS and may provide guidance for the selection of 1, 25$(OH)_2$ D_3 concentration and mechanical loading in order to *in vitro* produce functional bone tissues.

Key words: 1, 25-dihydroxyvitamin D_3, Fluid shear stress, Osteoblasts, The collective influence

bioRxiv preprint doi: https://doi.org/10.1101/146159; this version posted June 5, 2017. The copyright holder for this preprint (which was not certified by peer review) is the author/funder. All rights reserved. No reuse allowed without permission.

1. Introduction

1, 25-dihydroxyvitamin D_3 (1, 25 $(OH)_2$ D_3) is a kind of vitamin D active metabolite, which plays an important role in the pathogenesis of osteoporosis. The features of osteoporosis are low bone mass and bone microstructure destruction. Osteoporosis is a systemic metabolic bone disease and increased bone fragility and susceptibility to fracture. For the treatment of osteoporosis, vitamin D active metabolite has been applied widely. What's more, 1, 25-dihydroxyvitamin D_3 is one of the most widely applied vitamin D active metabolite and plays an significant role in the regulation of calcium and phosphate metabolism, also can obviously affect the proliferation, differentiation of osteoblasts[1-3]. The researchers found that 1, 25 $(OH)_2$ D_3 inhibits cell growth and enhances osteoblast differentiation by regulating the expression of collagenous and non-collagenous proteins, including osteocalcin and osteopontin[4, 5]. Further, M. Van Driel and V.J.Woeckel demonstrated that 1, 25 $(OH)_2$ D_3 can enhance the mineralization of osteoid tissue produced by osteoblasts[6, 7].Thus, Understanding the effects of 1, 25 $(OH)_2$ D_3 on the perception of osteoblasts is beneficial for the treatment of osteoporosis, inducing appropriate cell responses and promoting bone formation.

In addition, bone is a kind of porous dynamic tissue in the body. It is always subjected to a variety of mechanical stimulation from outside and inside. If the receiving force of bone is reduced, such as bedridden for a long time, bone fixation or a decrease in physical activity, which leads to increase the absorption of bone, severe bone loss, and enhance the risk of osteoporosis. The structure of bone may be caused and maintained

bioRxiv preprint doi: https://doi.org/10.1101/146159; this version posted June 5, 2017. The copyright holder for this preprint (which was not certified by peer review) is the author/funder. All rights reserved. No reuse allowed without permission.

by the difference between the actual receiving mechanical stimulation of bone and the mechanical amplitude of normal internal environment. At the level of cells, fluid shear stress (FSS) generated in canalicular systems of physiological bone is regarded as the principal mechanical stimulus responsible for bone adaption and remodeling[8-10]. As a result, FSS is widely employed as an external mechanical stimulus in bioreactors for bone tissue engineering[11, 12]. Various magnitudes of FSS from 10 dynes/cm^2 to 20 dynes/cm^2 have been concluded to influence the morphological responses, proliferation and differentiation of osteoblasts with a magnitude-dependent and duration-dependent manner[13-16]. Particularly, Liu et al[16] reported that stimulation of 16 dynes/cm^2 or 19 dynes/cm^2 FSS for 1h induced osteoblasts reorientation along FSS direction while 12 dynes/cm^2 FSS did not. Kapur[13] found that 20 dynes/cm^2 FSS for 30min obviously promoted osteoblasts proliferation and differentiation, while Horikawa[17] pointed out that long-term FSS stimulation such as 10 dynes/cm^2 for over 1h had destructive effects on osteoblasts. In bone tissue *in vivo*, the physiological FSS caused by interstitial fluid flow is 8~30 dynes/cm^2 on the basis of the model presented by Weinbaum[18]. In this study, 12 dynes/cm^2 were employed to represent physiological FSS.

The aim of this study is to investigate the collective effects of 1, 25 $(OH)_2$ D_3 with physiological fluid shear stress on osteoblasts. To this end, 1, 25 $(OH)_2$ D_3 were constructed in various kinds of concentration (0, 1, 10, 100 nmol/L), while physiological fluid shear stress (12 dynes/cm^2) were produced by using a parallel-plate fluid flow system. The plasma membrane integrity, the short-term

bioRxiv preprint doi: https://doi.org/10.1101/146159; this version posted June 5, 2017. The copyright holder for this preprint (which was not certified by peer review) is the author/funder. All rights reserved. No reuse allowed without permission.

response on releases of nitric oxide (NO) and prostaglandin E_2 (PGE_2) and the long-term response on cell proliferation (Proliferation index, PI), alkaline phosphatase (ALP), osteopontin (OPN) and osteocalcin (OCN), these all were selected to characterize the responses of osteobalst to collective stimulation. To elaborate the potential mechanism, the focal adhesions formation (FA) and cytoskeleton rearrangement (F-actin) before and after FSS stimulation were further examined. The cell morphology and orientation were quantified as well. Selection of NO and PGE_2 releases is based on the fact that they are the early rapid responses of osteoblasts to FSS and play important roles in bone formation and remodeling[19-22].

2. Materials and methods

2.1. Osteoblasts culture

Primary rat osteoblasts (ROBs) cultures were described in our previous paper[23]. Briefly, the calvaria bone of SD rats was removed and placed in petri dish containing PBS buffer. The periosteum and surrounding connective tissue were removed by using tweezers. The calvaria bone was washed with PBS and cleaned with DMEM until the surface of bone is white and transparent, immersed into a small amount of fetal calf serum. The calvaria bone was cut into about 1mm×1mm×1mm pieces, coated uniformly in 25ml culture flask. Cultures were initiated in DMEM (Gibico, USA) supplemented with 10% heat-inactivated fetal calf serum (FCS, Sijiqing, China), penicillin (100U/mL), streptomycin (100μg/mL), and 0.05% L-glutamine, and maintained in a humidified atmosphere of 5% CO_2/95% air at 37°C. The medium was

bioRxiv preprint doi: https://doi.org/10.1101/146159; this version posted June 5, 2017. The copyright holder for this preprint (which was not certified by peer review) is the author/funder. All rights reserved. No reuse allowed without permission.

changed every two days. After confluence, the cells were sub-cultured and identified by using the von Kossa staining method according to previously reported procedure[23]. The fourth to sixth passage of ROBs were used for experiments at a density of 2×10^5 cells/slide.

2.2. Physiological fluid shear stress and static treatments

A parallel-plate flow chamber apparatus was employed to provide FSS[24]. The dimension of the flow chamber was 7.50cm (length, L) × 2.50 cm (width, W) × 0.03cm (height, H). FSS was produced by circulating 10 mL DMEM using a peristaltic pump (JieHeng, China). The produced FSS (τ, dynes/cm^2) was calculated according to equation $\tau = 6\eta Q / H^2 W$, where η is the dynamic viscosity of the perfusate and Q is the flow rate. To study the collective effects of 1, 25 $(OH)_2 D_3$ and FSS on the responses of osteoblasts, pre-incubations of ROBs for 24h were performed in medium with 1, 25 $(OH)_2 D_3$ (0, 1, 10, 100 nmol/l) (Sigma–Aldrich, USA) under static conditions. The concentrations of 1, 25 $(OH)_2 D_3$ were chosen based on a previous study in which the different concentration of 1, 25 $(OH)_2 D_3$ affected osteoblast proliferation and differentiation to a similar extend[5, 25, 26]. Thereafter, osteoblasts were subjected to FSS or static treatment asdescribed previously[27]. Shortly, the employed physiological FSS in this study was 12 dynes/cm^2. All the components of the apparatus, except the pump, were maintained in a 37°C incubator during the experiment and the medium was continuously saturated with 5% CO_2/95% air. For FSS-loaded samples (denoted by X-FSS, where X represents different concentration of 1, 25 $(OH)_2 D_3$), slides with attached ROBs were first mounted on

bioRxiv preprint doi: https://doi.org/10.1101/146159; this version posted June 5, 2017. The copyright holder for this preprint (which was not certified by peer review) is the author/funder. All rights reserved. No reuse allowed without permission.

the flow chamber and then exposed to FSS for a predetermined time. Other samples without FSS exposure (denoted by X-Static) were kept in Petri dishes at 37°C in a humidified atmosphere of 5% CO_2/95% air for the same predetermined time.

2.3. Determination of NO, and PGE_2 releases

After incubation with 1, 25 $(OH)_2$ D_3 for 24h, ROBs were employed for the determination of NO, and PGE_2 releases. After ROBs on slides were exposed to FSS for a predetermined time, 2 mL of medium was withdrawn and replenished with an equal volume of fresh culture medium to maintain a constant circulating fluid volume. The same procedure was performed for samples without FSS exposure.

2.3.1. NO release

NO concentration was detected by using a Nitric Oxide Assay Kit (Beyotime, China) based on Griess Reagent. The withdrawn medium was permitted to react with Griess Reagent for 10 min, and then the absorbance was measured at 540nm using a Microplate Reader (Bio-Rad, USA). The NO concentration was determined according to the standard curve plotted by the supplied $NaNO_2$ standards and normalized to the total cellular protein.

2.3.2. PGE_2 release

PGE_2 release was measured by using a Rat PGE_2 ELISA Assay Kit (Yuan-Ye Chemical reagents, China).The absorbance was detected at 450nm and the PGE_2 concentration was determined on the basis of the standard curve plotted by the

bioRxiv preprint doi: https://doi.org/10.1101/146159; this version posted June 5, 2017. The copyright holder for this preprint (which was not certified by peer review) is the author/funder. All rights reserved. No reuse allowed without permission.

supplied PGE_2 standards and normalized to the total cellular protein.

2.4. Determination of the proliferative index (PI)

After being exposed to FSS for 1 h, the cells were trypsinized, washed with PBS, and fixed in 70% ethanol at 4°C.The cell suspension was centrifuged at 2000r/min for 10min. The collected ROBs were washed with PBS and then 1mL of PBS was added to obtain the cell suspension again. Following this, 20 μL of RNAse (10 mg/mL) was added to the obtained cell suspension and it was then incubated at 37°C for at least 30min. Then, 50μL of pyridine iodide was added to the cell suspension and it was incubated in the dark at 37°C for another 30 min. Finally, the cell cycle stages were detected using a Flow Cytometry (BD FACS Vantage SE, USA) and analyzed using Cell quest software (Becton Dickinson). The cell proliferative index (PI%) was calculated using the following formula: $PI\% = [(S + G2/M) / (G0/G1 + S + G2/M)]\%$, where S, G2/M, and G0/G1 represent the cell numbers in phase S, phase G2 and M, and phase G0 and G1, respectively, in cell cycle.

2.5. Plasma membrane integrity after FSS exposure

Lactate dehydrogenase (LDH) level released from cytoplasma is a common parameter to indicate the integrity of plasma membrane[28]. After exposure of ROBs to FSS for 1 h, 500 μL of the conditioned medium was employed for detection of LDH level by using a LDH Assay Kit (Jiancheng, China). The basic principle of this assay is that NADH, generated by oxidization of lactate into pyruvate under the catalysis of

bioRxiv preprint doi: https://doi.org/10.1101/146159; this version posted June 5, 2017. The copyright holder for this preprint (which was not certified by peer review) is the author/funder. All rights reserved. No reuse allowed without permission.

LDH, may convert iodonitrotetrazolium into a red formazan product in the presence of diaphorase. The absorbance of formazan at 490 nm is proportional to the amount of LDH in the medium. Comparison of the LDH level with FSS exposure to that without FSS exposure may indicate the integrity of plasma membrane.

2.6. Focal adhesions and cytoskeletons of ROBs before and after FSS exposure

Focal adhesion formation and cytoskeleton rearrangement of ROBs before and after 1h FSS exposure were examined by immunofluorescence staining. Before staining, ROBs were fixed through incubation in 4% (w/v) paraformaldehyde in PBS for 30 min and permeabilized for 10 min with 0.25% (v/v) Triton X-100 in PBS. Subsequently, 1% BSA in PBS was added to block the non-specific binding sites by incubating with ROBs for 1h. To observe focal adhesion formation, vinculin was stained by initially incubating with a mouse monoclonal anti-vinculin antibody at room temperature for 60 min, and subsequently incubating with a FITC-conjugated anti-mouse immunoglobulin secondary antibody at room temperature for another 60min. F-actin was stained using Rhodamine-Phalloidin at room temperature for 60 min. Finally, the nuclei were stained by incubation with bisBenzimide H 33258 at room temperature for 10min. The stained specimens were washed, mounted in glycerol, and examined by a confocal laser scanning microscope (CLSM; TCS SP5, Leica, Germany).

bioRxiv preprint doi: https://doi.org/10.1101/146159; this version posted June 5, 2017. The copyright holder for this preprint (which was not certified by peer review) is the author/funder. All rights reserved. No reuse allowed without permission.

2.7. ALP assay

ROBs were exposed to FSS for 1 h, the ROBs were collected and lysed for 30 min in 150 μL lysis buffer (Cwbiotech, China) on ice. The total proteins were got in supernatants with centrufugation (14000 r/min). The ALP activity was detected by ALP assay kit (Nanjing Jiancheng Bioengineering Institute, China). The total protein concentration, detected by BCA Protein Assay Kit (Beyotime, China), was used to normalize ALP activity. The absorbance was detected by Multifunctional Microplate Reader (Bio-Rad) at 490 nm and 570 nm for ALP and BCA analysis, respectively.

2.8. Quantitative real-time polymerase chain reaction (qRT-PCR)

After exposure to FSS for 1 h, the differentiation of osteoblasts stimulated with both 1, 25 $(OH)_2$ D_3 and FSS was further assessed by qRT-PCR. The relative mRNA expression levels of commonly used bone markers, including osteopontin (OPN) and osteocalcin (OCN) (primer pairs used are shown in Table 1), were measured. Total RNA isolation for qRT-PCR samples was conducted using an RNA simple Total RNA Kit (Biotake, Beijing, China). Complementary DNA (cDNA) was then reversetranscribed from 1 mg of total RNA using a RevertAid First Strand cDNA Synthesis Kit (ThermoFisher Scientific, USA) according to manufacturer instructions. Realtime PCR was performed on SYBR Green PCR Master Mix (T advanced, JENA, Germany) and the reaction was carried out using an ABI 7500 system (Scandrop, JENA, Germany). Finally, housekeeping gene glyceraldehyde-3-phosphate dehydrogenase (GAPDH) was used to normalize therelative mRNA expression level

bioRxiv preprint doi: https://doi.org/10.1101/146159; this version posted June 5, 2017. The copyright holder for this preprint (which was not certified by peer review) is the author/funder. All rights reserved. No reuse allowed without permission.

of each gene and quantification was based on the cycle threshold (CT) values.

Gene	Forward primer (5'–3')	Reverse primer (5'–3')	Accession no.
GAPDH	GGCACAGTCAAGGCTGAGAATG	ATGGTGGTGAAGACGCCAGTA	NM 017008.4
OPN	CCAAGCGTGGAAACACACAGCC	GGCTTTGGAACTCGCCTGACTG	M14656.1
OCN	GGTGCAGACCTAGCAGACACCA	AGGTAGCGCCGGAGTCTATTCA	J04500

Table 1 OPN and OCN used in PCR analysis

2.9. Statistical analysis

Data were expressed as means ± SD (n ≥6 for all experiments). Single factor analysis of variance (ANOVA) technique with OriginPro (version 8.0) was used to assess the statistical significance of results. The confidence interval was set to 0.05.

3. Results

3.1. NO and PGE_2 releases

First, we examined the effects of 1, 25 $(OH)_2 D_3$ alone on the NO and PGE_2 releases of ROBs. As shown in Fig. 1, when no FSS was applied, ROBs released a small amount of NO (Fig. 1) and PGE_2 (Fig. 3). All the releases demonstrated no observable change with incubation time. This implies that 1, 25 $(OH)_2 D_3$ alone has negligible effects on NO and PGE_2 releases of ROBs. When FSS was applied, the NO and PGE_2 releases were significantly increased compared to their corresponding static counterparts (Fig. 1-3). Nevertheless, 10-FSS and 100-FSS had and obvious decrease in NO releases compared to the 0-FSS and 1-FSS, also 0-FSS ≈ 1-FSS (Fig. 2). But the opposite phenomena were observed for PGE_2 releases (Fig. 3). It is seen that FSS

bioRxiv preprint doi: https://doi.org/10.1101/146159; this version posted June 5, 2017. The copyright holder for this preprint (which was not certified by peer review) is the author/funder. All rights reserved. No reuse allowed without permission.

induced significant increase PGE_2 releases (Fig. 3). This suggests that FSS-induced NO and PGE_2 releases of ROBs are 1, 25 $(OH)_2 D_3$ concentration dependent with a pattern of 0-FSS > 1-FSS > 10-FSS > 100-FSS for NO (Fig. 2), and 100-FSS > 10-FSS > 0-FSS ≈ 1-FSS for PGE_2 (Fig. 3).

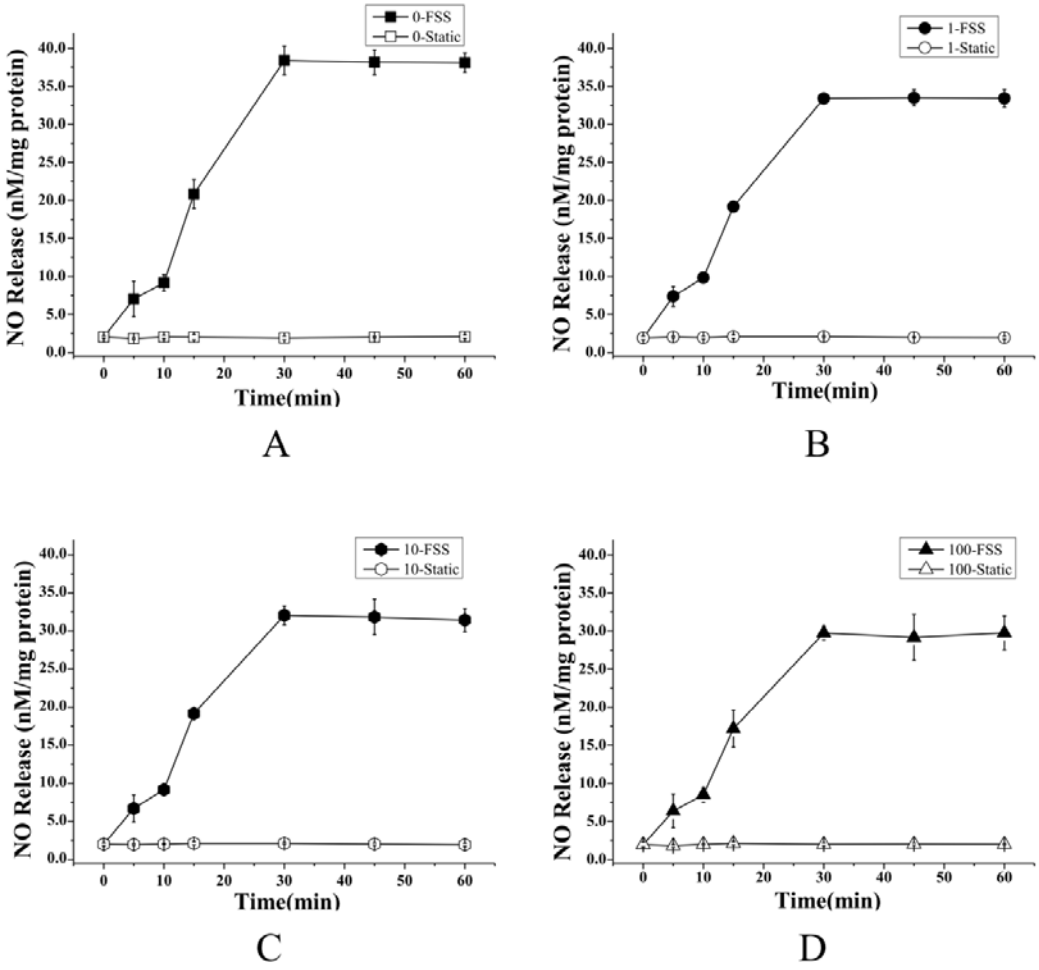

Fig. 1 Releases of NO with different 1, 25 $(OH)_2 D_3$ concentration for Static and FSS.

bioRxiv preprint doi: https://doi.org/10.1101/146159; this version posted June 5, 2017. The copyright holder for this preprint (which was not certified by peer review) is the author/funder. All rights reserved. No reuse allowed without permission.

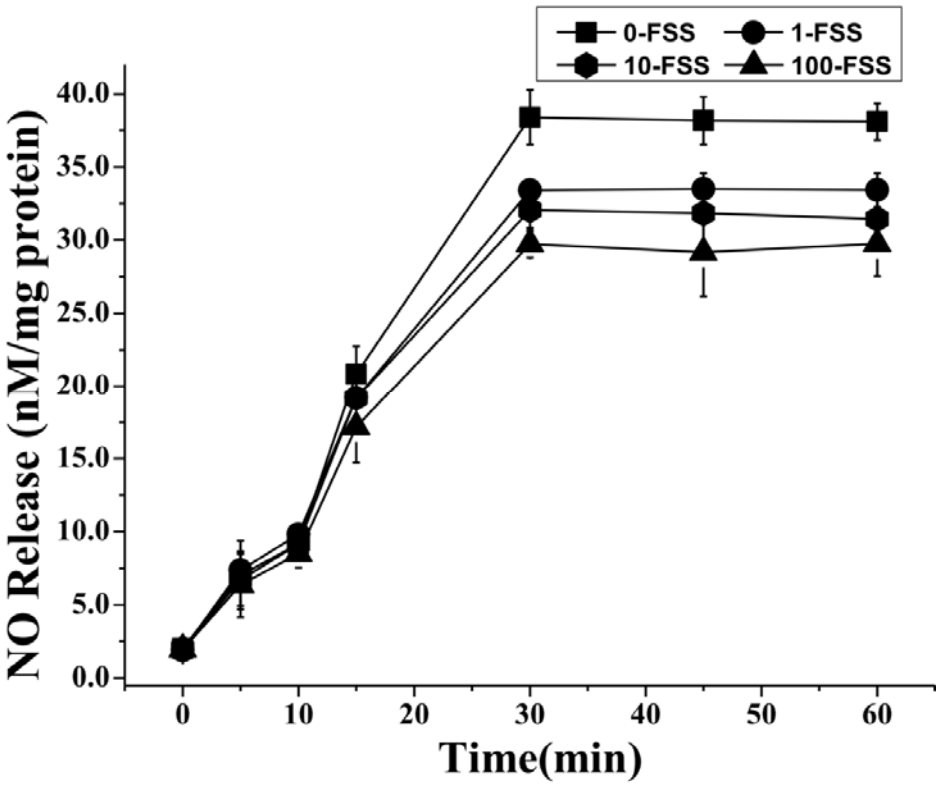

Fig. 2 Releases of NO with different 1, 25 $(OH)_2$ D_3 concentration for FSS.

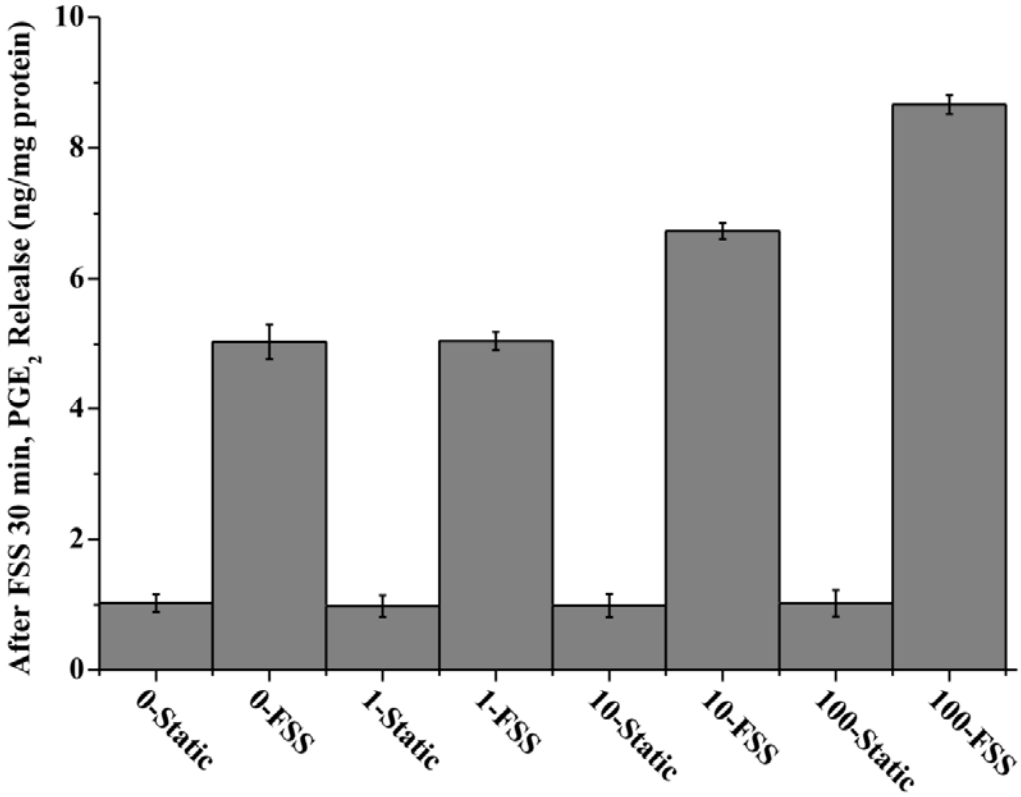

Fig. 3 Releases of PGE_2 with different 1, 25 $(OH)_2$ D_3 concentration for Static and FSS.

bioRxiv preprint doi: https://doi.org/10.1101/146159; this version posted June 5, 2017. The copyright holder for this preprint (which was not certified by peer review) is the author/funder. All rights reserved. No reuse allowed without permission.

3.2. Determination of the proliferative index (PI)

The cell proliferation potential can be indicated by cell proliferative index (PI), which is the ratio of cell number in G2/M phase and S phase to the total cell number. The PI values of ROBs incubated by 1, 25 $(OH)_2 D_3$, without or with FSS exposure, were determined by using flow cytometry and the result is illustrated in Fig. 4. The typical histograms of the PI cell-cycle profiles are shown in Fig. 5. It is clear that 1, 25 $(OH)_2 D_3$ inhibited ROBs proliferation, and the stronger concentration of 1, 25 $(OH)_2 D_3$, the stronger inhibition. But after applying FSS, the PI of all X-FSS is increased, and higher than those of 0-Static, which indicates that the exposure of FSS counteracts the inhibitory effect of 1, 25 $(OH)_2 D_3$ on ROBs proliferation. The PI values for ROBs exposed to various concentrations of 1, 25 $(OH)_2 D_3$ and FSS were shown in Fig. 4 and followed the pattern 0-FSS > 10-FSS > 1-FSS > 100-FSS.

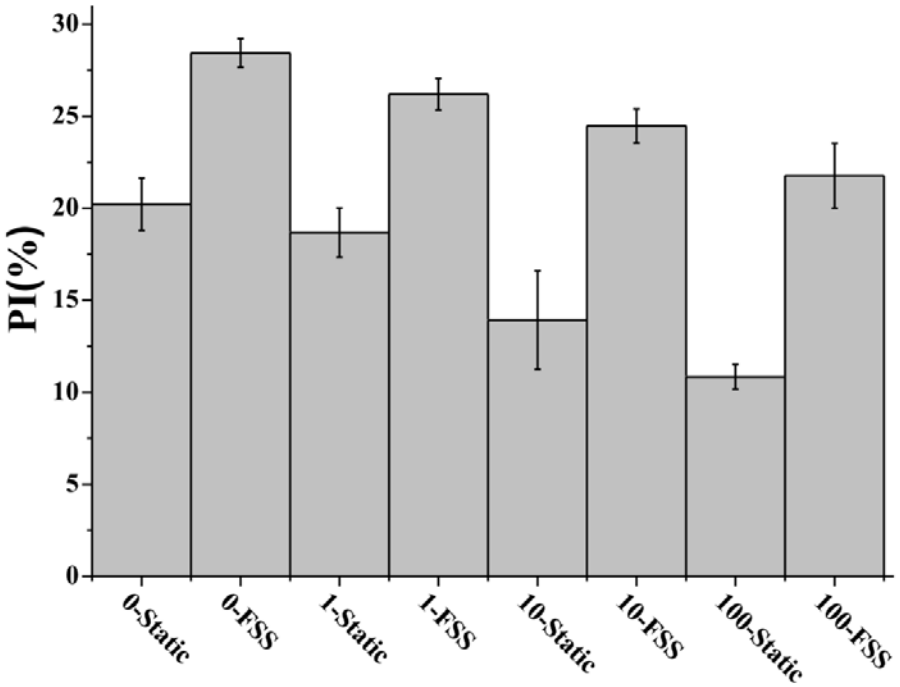

Fig. 4 PI values of ROBs with different 1, 25 $(OH)_2 D_3$ concentration for Static and FSS.

bioRxiv preprint doi: https://doi.org/10.1101/146159; this version posted June 5, 2017. The copyright holder for this preprint (which was not certified by peer review) is the author/funder. All rights reserved. No reuse allowed without permission.

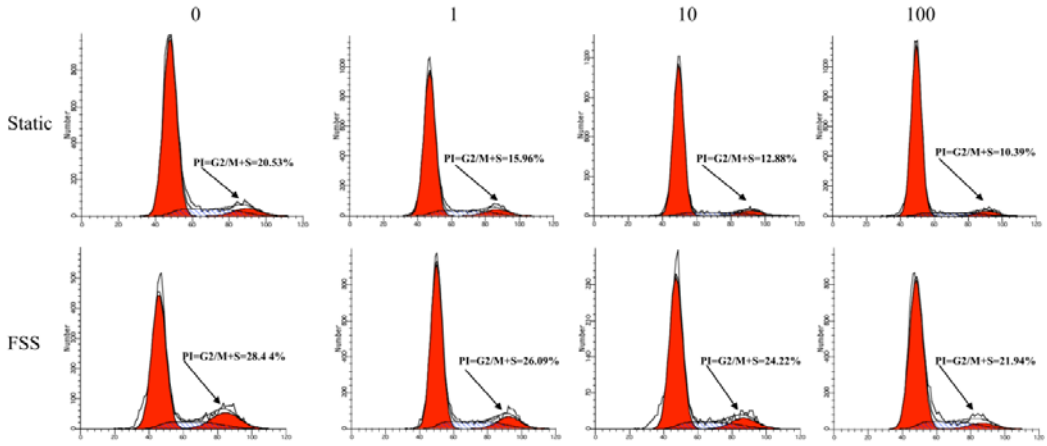

Fig. 5 Representative histograms of the PI cell-cycle profiles.

3.3. Plasma membrane integrity after FSS exposure

To make sure whether the detected NO and PGE_2 are actively released by ROBs in response to FSS or passively released due to plasma membrane rupture by FSS, the plasma membrane integrity was monitored by detecting the LDH level in the conditioned media. The ratio of LDH level with FSS exposure to that without FSS exposure was employed to evaluate the plasma membrane integrity. As can be seen from Fig. 6, the LDH ratios for all of FSS-induced ROBs are close to 1. This indicates that the plasma membranes are intact and all NO and PGE_2 for X-FSS (X=0, 1, 10, 100) are actively released by ROBs.

bioRxiv preprint doi: https://doi.org/10.1101/146159; this version posted June 5, 2017. The copyright holder for this preprint (which was not certified by peer review) is the author/funder. All rights reserved. No reuse allowed without permission.

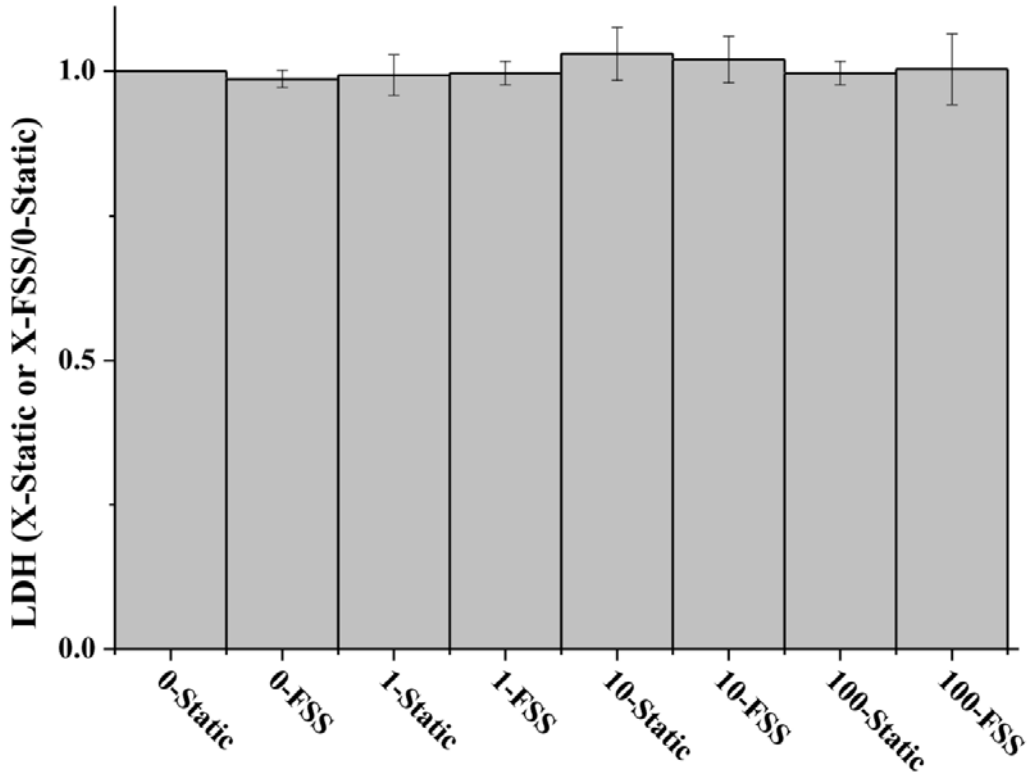

Fig. 6 The ratio of LDH release induced for Static and FSS.

3.4. Focal adhesions, cytoskeletons and morphologies of ROBs before and after FSS

To elucidate the possible mechanism by which different concentration induces different responses of ROBs to FSS, the focal adhesion formation, F-actin organization and morphologies of ROBs before and after FSS exposure were examined and pictured using a CLSM. The typical pictures were shown in Fig. 7, where the blue, green, and red represent nuclei, vinculin, and F-actin, respectively. Based on the fluorescence images, the cell aspect ratios and angles between cell axis and FSS direction were further measured by using Image J software to quantify cell shape and orientation (Table. 2 and 3). ROBs with an angle of 0-30° are referred to

bioRxiv preprint doi: https://doi.org/10.1101/146159; this version posted June 5, 2017. The copyright holder for this preprint (which was not certified by peer review) is the author/funder. All rights reserved. No reuse allowed without permission.

"oriented along FSS direction" while those with an aspect ratio of 1-3 and > 3 are referred to "spread" and "elongated" shape, respectively.

Before FSS exposure, 10-Static, and 100-Static spread batter and contained a larger number of focal adhesions and more clear F-actin stress fibers than 0-Static; nevertheless, 1-Static displayed few focal adhesions and vague F-actin stress fibers (Fig. 7). Judging from the cell aspect ratio (Table. 2), 0-Static, 10-Static and 100-Static were spread (62.33%, 70.86% and 72.12% of ROBs with a cell aspect ratio of 1-3) whereas 1-Static were elongated (75.18% of ROBs with a cell aspect ratio of > 3). Regarding cell orientation, ROBs percentages taking an angle of 0°-30°, 30°-60° and 60°-90° are comparable on all of samples, suggesting random orientation of ROBs (Table. 3).

After 1 h of FSS exposure, the percentage of ROBs taking an angle of 0°-30° dramatically increased for all samples (for 0 from 32.42% to 75.18%, for 1 from 34.76% to 71.34%, for 10 from 35.69% to 77.42% and for 100 from 32.31% to 74.87%) (Table. 3). ROBs present a partially oriented morphology along the FSS direction. At the same time, all samples despite a slight decrease in ROBs percentage taking an aspect ratio of 1-3 except 1 (for 0 from 62.33% to 65.89%, for 10 from 70.86% to 77.24% and for 100 from 72.12% to 76.92%) (Table. 2). The cell aspect ratios and angles suggest that FSS induced obvious cell reorientation and slight shape alteration.

bioRxiv preprint doi: https://doi.org/10.1101/146159; this version posted June 5, 2017. The copyright holder for this preprint (which was not certified by peer review) is the author/funder. All rights reserved. No reuse allowed without permission.

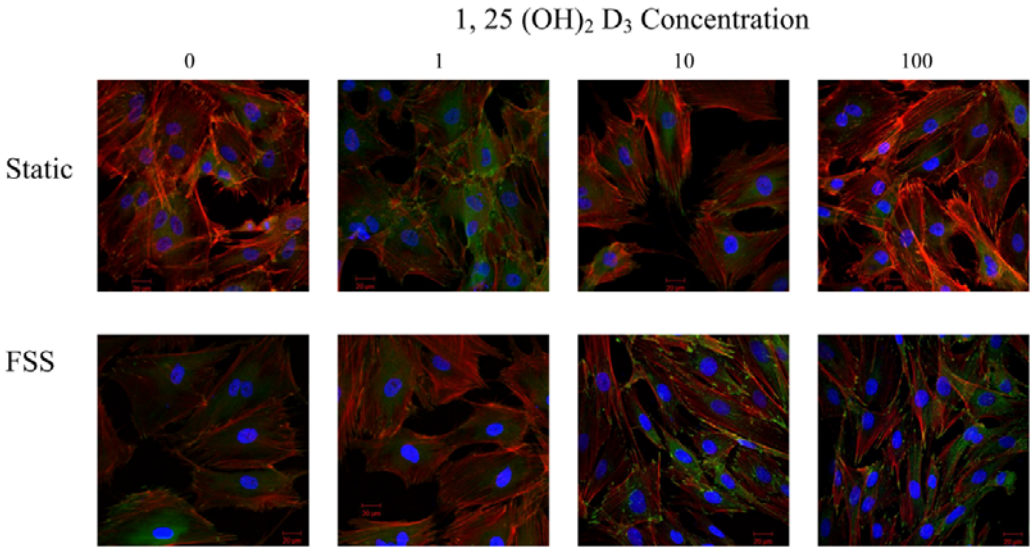

Fig. 7 Focal adhesion and F-actin formation of ROBs with different 1, 25 $(OH)_2$ D_3 concentration for Static and FSS. ROBs were fixed, permeabilized, and double labeled for vinculin (green), F-actin (red), and nuclei (blue). The yellow areas are vinculin, partially colocalized with F-actin in the focal adhesion plaques.

1, 25 $(OH)_2$ D_3 Concentration	Percentage (%)					
	1-3		3-5		>5	
	Static	FSS	Static	FSS	Static	FSS
0	62.33	65.89	30.12	27.66	7.55	6.45
1	24.82	21.22	66.39	76.91	8.79	1.87
10	70.86	77.24	29.14	22.76	0	0
100	72.12	76.92	27.88	21.71	0	1.37

Table 2 Cell aspect ratios with different 1, 25 $(OH)_2$ D_3 concentration for Static and FSS

bioRxiv preprint doi: https://doi.org/10.1101/146159; this version posted June 5, 2017. The copyright holder for this preprint (which was not certified by peer review) is the author/funder. All rights reserved. No reuse allowed without permission.

1, 25 $(OH)_2 D_3$ Concentration	Percentage (%)					
	0°-30°		30°-60°		60°-90°	
	Static	FSS	Static	FSS	Static	FSS
0	32.42	75.18	29.44	20.92	38.14	3.90
1	34.76	71.34	31.58	22.63	33.66	6.03
10	35.69	77.42	29.46	19.85	34.85	2.73
100	32.31	74.87	37.15	23.69	30.54	1.44

Table 3 Cell orientation with different 1, 25 $(OH)_2 D_3$ concentration for Static and FSS

3.5. ALP analysis

ALP will significantly increase during the post proliferative phase of osteoblasts, and it's an early marker for differentiation[29]. The ALP activity of ROBs by treated with various concentration 1, 25 $(OH)_2 D_3$ and (with or without) FSS for 1 h are shown in Fig. 8, respectively. As we can see that 10-Static and 100-Static enhanced ALP activity of ROBs compared to 0-Static, and 100-Static > 10-Static, which suggests that 10nmol/L and 100nmol/L 1, 25 $(OH)_2 D_3$ promote ROBs differentiation. On the contrary, ALP activity of 1-Static is slightly decreased, and lower than those of 0-Static, which indicates that 1nmol/L 1, 25 $(OH)_2 D_3$ has a negligible inhibition to ROBs differentiation. After ROBs exposed to FSS for 1h, the ALP activity of 1-FSS is increased, and higher than those of 0-Static, which indicates that the exposure of FSS counteracts the inhibitory effect of 1, 25 $(OH)_2 D_3$ on ROBs differentiation. What's more, ALP activity of 10-FSS and 100-FSS has a significant increase in contrast to 10-Static and 100-Static. The ALP activity of ROBs exposed to various concentrations of 1, 25 $(OH)_2 D_3$ and FSS followed the pattern 100-FSS > 10-FSS > 0-FSS > 1-FSS.

bioRxiv preprint doi: https://doi.org/10.1101/146159; this version posted June 5, 2017. The copyright holder for this preprint (which was not certified by peer review) is the author/funder. All rights reserved. No reuse allowed without permission.

It is in good agreement with the suppressed cell proliferation (Fig. 4) which generally increases cell differentiation[25, 30].

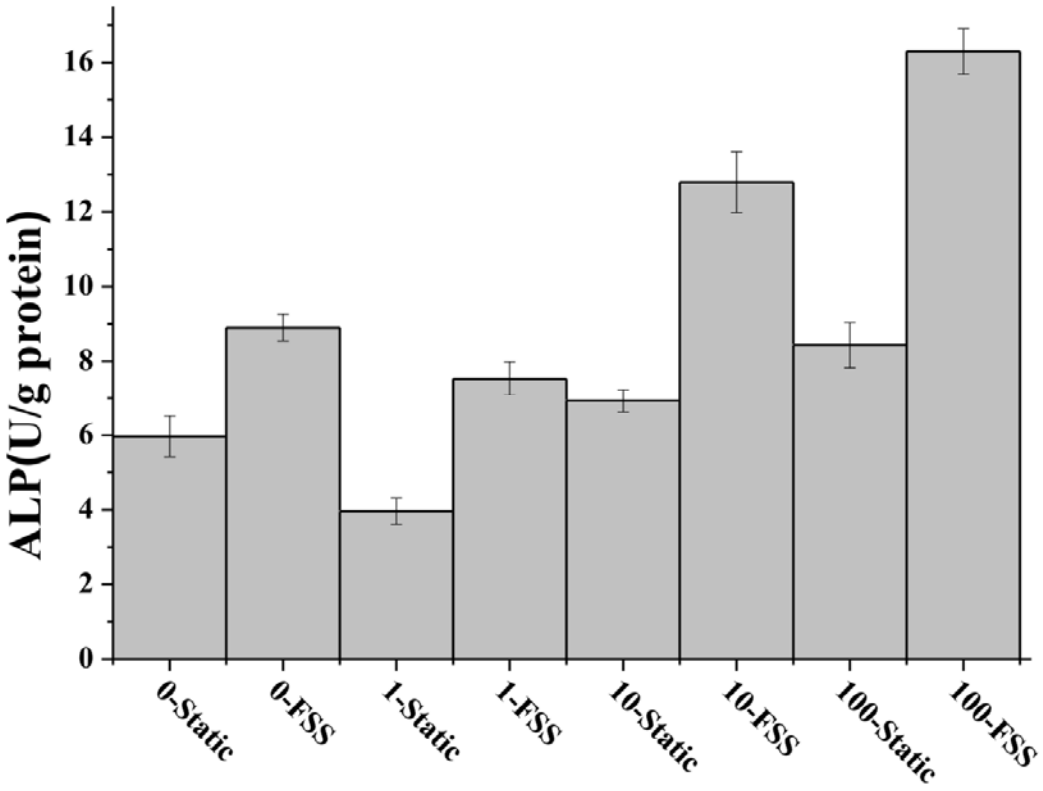

Fig. 8 ALP activity of ROBs with different 1, 25 $(OH)_2$ D_3 concentration for Static and FSS.

3.6. Quantitative real-time polymerase chain reaction (qRT-PCR)

Fig. 9 summarizes the differentiation-related gene expressions of OPN, OCN for all samples. It is similar to ALP analysis that 10-Static and 100-Static enhanced OPN and OCN gene expressions of ROBs compared to 0-Static, and 100-Static > 10-Static. However, OPN and OCN gene expressions of 1-Static are the same as 0-Static without variation. After ROBs exposed to FSS for 1h, OPN and OCN of 1-FSS is increased, and higher than those of 0-Static, which indicates that FSS enhanced OPN and OCN gene expressions of ROBs by 1nmol/L 1, 25 $(OH)_2$ D_3 treatment. Moreover,

bioRxiv preprint doi: https://doi.org/10.1101/146159; this version posted June 5, 2017. The copyright holder for this preprint (which was not certified by peer review) is the author/funder. All rights reserved. No reuse allowed without permission.

OPN and OCN gene expressions of 10-FSS and 100-FSS has a significant increase in contrast to 10-Static and 100-Static. The OPN and OCN gene expressions of ROBs exposed to various concentrations of 1, 25 $(OH)_2 D_3$ and FSS followed the pattern 100-FSS > 10-FSS > 1-FSS ≈ 0-FSS (Fig. 9).

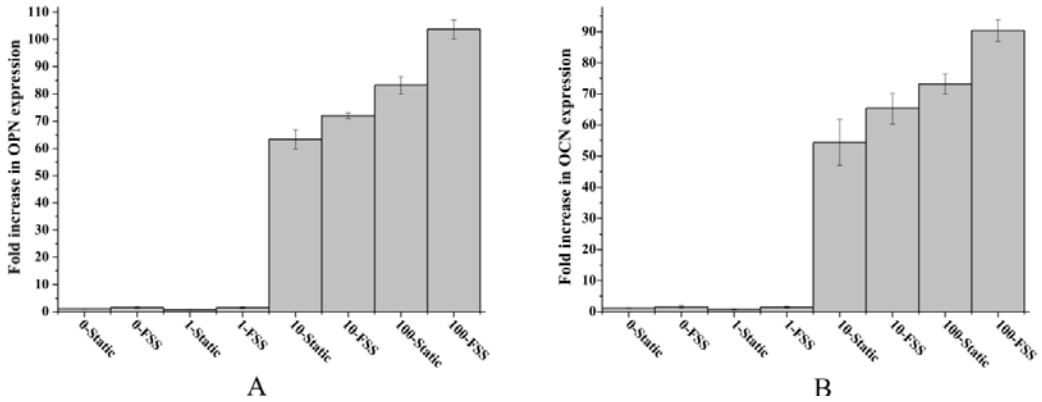

Fig. 9 OPN and OCN expression of ROBs with different 1, 25 $(OH)_2 D_3$ concentration for Static and FSS.

4. Discussion

The aim of this study was to find the collective effects of 1, 25 $(OH)_2 D_3$ with physiological fluid shear stress on osteoblasts, and to understand the possible mechanism of these responses. 1, 25-dihydroxyvitamin D_3 and mechanical stimuli are extremely important components for bone tissue engineering. FSS is the principle mechanical stimulus responsible for physiological bone modeling/remodeling[8-10] and thus often employed as an external mechanical stimulus in researching osteobalsts[31-33]. In this study, we found that the different concentration of 1, 25 $(OH)_2 D_3$ regulates the responses of osteoblasts to FSS, with the better responses on 10-FSS and 100-FSS yet the worse responses on 1-FSS, than 0-FSS. The potential

bioRxiv preprint doi: https://doi.org/10.1101/146159; this version posted June 5, 2017. The copyright holder for this preprint (which was not certified by peer review) is the author/funder. All rights reserved. No reuse allowed without permission.

mechanism is that 1, 25 $(OH)_2 D_3$ modulates the focal adhesions and cytoskeletons which further leads to differential alteration in cell short term responses such as signal molecular (NO and PGE_2) release, shape, orientation, and long term responses of ALP, PI, and gene expressions such as OPN and OCN after exposed to FSS.

The releases of NO and PGE_2 are known to play an important role in bone formation and remodeling, and they are essential early responses of osteoblasts to FSS[34-36]. In this light, NO and PGE_2 releases were selected as parameters to indicate the early responses of ROBs. It is not consistent with previous studies about Alone-FSS-induced release of NO[37-40], the collective effects of 1, 25 $(OH)_2 D_3$ with FSS inhibited NO release of ROBs (Fig. 1 and Fig. 2). However, the inhibition of pre-incubation with 1, 25 $(OH)_2 D_3$ to FSS-induced NO release was reported and in line with some previous literatures[40, 41]. On the contrary, pre-incubation with 1, 25 $(OH)_2 D_3$ promoted obviously PGE_2 release of ROBs to FSS, which shown a concentration dependence of 1, 25 $(OH)_2 D_3$ with a pattern of 100-FSS > 10-FSS > 0-FSS > 1-FSS (Fig. 3). Therefore, one conclusion could be made that 1, 25 $(OH)_2 D_3$ inhibited FSS-induced NO release of ROBs, and this inhibition was concentration dependent, the stronger concentration of 1, 25 $(OH)_2 D_3$, the stronger inhibition. At the same time, the high concentration (10nmol/L and 100nmol/L) can promote FSS-induced PGE_2 release, and low concentration (1nmol/L) reduced.

Furthermore, cell proliferation and differentiation as a long-term response of ROBs was further investigated to evaluate the synergistic effect of 1, 25 $(OH)_2 D_3$ and FSS by using PI, ALP activity, gene expressions of OPN and OCN. We found the same

bioRxiv preprint doi: https://doi.org/10.1101/146159; this version posted June 5, 2017. The copyright holder for this preprint (which was not certified by peer review) is the author/funder. All rights reserved. No reuse allowed without permission.

phenomenon that 1, 25 $(OH)_2 D_3$ inhibits osteoblast proliferation consistent with the report of K. Van der Meijden[5]. More importantly, the inhibitory effect was concentration dependent like 0-Static > 1-Static> 10-Static> 100-Static (Fig. 4 and Fig. 5). In addition, the addition of FSS eliminated a part of this inhibition, demonstrating that 1-FSS > 0-Static, 10-FSS > 0-Static, 100-FSS > 0-Static (Fig. 4 and Fig. 5). From the perspective of cell differentiation, 1nmol/L 1, 25 $(OH)_2 D_3$ has little effect on ALP activity, OPN and OCN gene expressions, but the addition of FSS appear a remarkable increase for these parameters. This phenomenon illustrates that low concentration of 1, 25 $(OH)_2 D_3$, such as 1nmol/L, could not promote cell differentiation. However, 1-FSS has a remarkable increase on cell differentiation, which shows that FSS plays a dominant role on the synthesis of 1nmol/L 1, 25 $(OH)_2 D_3$ and FSS in cell differentiation. Additionally, the high concentration of 1, 25 $(OH)_2 D_3$ (1nmol/L and 10nmol/L) can promote cell differentiation, and this effect is further enhanced by the intervention of FSS (Fig. 8 and Fig. 9).

Initial adhesion and spreading of osteoblasts, including integrin-medicated cytoskeleton rearrangement[20-22, 42, 43] and initial formation of FA[44-47], have been regarded as critical factors that influence FSS-related mechanotransduction. Pavalko *et al.* proved that FSS-induced mechanical signaling in MC3T3-E1 osteoblasts requires cytoskeleton-integrin interactions[48]. However, McGarry *et al.* disrupted the cytoskeleton of osteoblasts and found that FSS-induced NO releases need intact actins, whereas PGE_2 releases are independent on actin cytoskeleton reorganization[49]. In addition, Ponik and Pavalko used bovine serum albumin and RGDS to inhibit

bioRxiv preprint doi: https://doi.org/10.1101/146159; this version posted June 5, 2017. The copyright holder for this preprint (which was not certified by peer review) is the author/funder. All rights reserved. No reuse allowed without permission.

formation of focal adhesions in different degrees and confirmed that the releases of FSS-induced osteoblast PGE_2 are controlled by focal adhesion[50]. Taking all above information in mind, one hypothesis could be made that FA and F-actin organization should be responsible for the collective influence of 1, 25-dihydroxyvitamin D_3 with physiological fluid shear stress on osteoblasts.

To verify this hypothesis, FA and F-actin before FSS exposure were pictured (Fig. 7). The trend of F-actin is 100-Static > 10-Static > 1-Static ≈ 0-Static, while that of the FAs is 100-Static > 10-Static > 1-Static ≈ 0-Static. The common influences of FSS and 1, 25 $(OH)_2 D_3$ revealed that the PGE_2 releases, ROBs proliferation, ALP activity and gene expressions of OPN and OCN followed the similar patterns of FAs or F-actin organization. These results imply that 1, 25 $(OH)_2 D_3$ regulates the responses of ROBs to FSS by controlling the formation of FA and the organization of F-actin. 100nmol/L1, 25 $(OH)_2 D_3$ produced the best FAs and F-actin organization, so that the optimal combination of 1, 25 $(OH)_2 D_3$ with 12 dynes/cm^2 physiological FSS was observed on 100nmol/L1, 25 $(OH)_2 D_3$.

In summary, 1, 25 $(OH)_2 D_3$ affects the response of ROBs to FSS, including the inhibition of NO releases and cell proliferation as well as the promotion of PGE_2 releases and cell differentiation. These findings provide a possible mechanism by which 1, 25 $(OH)_2 D_3$ influences osteoblasts responses to FSS and may provide guidance for the selection of 1, 25 $(OH)_2 D_3$ concentration and mechanical loading in order to *in vitro* produce functional bone tissues.

bioRxiv preprint doi: https://doi.org/10.1101/146159; this version posted June 5, 2017. The copyright holder for this preprint (which was not certified by peer review) is the author/funder. All rights reserved. No reuse allowed without permission.

Acknowledgements

This work was supported by Grants from the Science and technology support program of Taizhou (No. TS301637), and Innovative Research Team of Taizhou polytechnic college (No. TZYTD-16-4).

References

[1] Maryam Doroudi, Marc C. Plaisance, Barbara D. Boyana, Zvi Schwartz. Membrane actions of 1a, 25$(OH)_2D_3$ are mediated by Ca^{2+}/calmodul independent protein kinase II in bone and cartilage cells. Journal of Steroid Biochemistry & Molecular Biology . 2014; 145: 65–74.

[2] Yong Hu, YangLiu, Daniel Lajeunesse, Didier Mainard, Jean-Yves Jouzeau, Pascal Reboul. Identification of two populations of osteoarthritic osteoblasts according to the 1, 25$[OH]_2$ vitamin D_3 potency to stimulate osteocalcin. Bio-Medical Materials and Engineering. 2015;25: S103–S110.

[3] Jason Peter Mansell, David Farrar, Scott Jones, Maryam Nowghani. Cytoskeletal reorganisation, 1, 25-dihydroxy vitamin D3 and human MG63 osteoblast maturation. Molecular and Cellular Endocrinology. 2009; 305: 38–46.

[4] A. Staal, G.J. Van den Bemd, J.C. Birkenhager, H.A. Pols, J.P. Van Leeuwen, Consequences of vitamin D receptor regulation for the 1,25-dihydroxyvitaminD3-induced 24-hydroxylase activity in osteoblast-like cells: initiation of the C24-oxidation pathway. Bone . 1997; 20: 237–243.

[5] K. Van der Meijden, P. Lips, M. Van Driel, A.C. Heijboer, E.A. Schulten, M. DenHeijer, N. Bravenboer. Primary human osteoblasts in response to 25-hydroxyvitamin D_3, 1,25-dihydroxyvitamin D_3 and 24R,25-dihydroxyvitamin D_3, PLoS One. 2014:10283.

bioRxiv preprint doi: https://doi.org/10.1101/146159; this version posted June 5, 2017. The copyright holder for this preprint (which was not certified by peer review) is the author/funder. All rights reserved. No reuse allowed without permission.

[6] M. Van Driel, M. Koedam, C.J. Buurman, M. Roelse, F. Weyts, H. Chiba, A.G. Uitterlinden, H.A. Pols, J.P. Van Leeuwen. Evidence that both 1a, 25-dihydroxyvitamin D_3 and 24-hydroxylated D_3 enhance human osteoblast differentiation and mineralization, J. Cell. Biochem. 2006; 99: 922–935.

[7] V.J. Woeckel, R.D. Alves, S.M. Swagemakers, M. Eijken, H. Chiba, B.C. van der Eerden, J.P. Van Leeuwen, 1a,25-$(OH)_2D_3$ acts in the early phase of osteoblast differentiation to enhance mineralization via accelerated production of mature matrix vesicles. J. Cell. Physiol. 2010; 225: 593–600.

[8] Hillsley MV, Frangos JA. Bone tissue engineering: the role of interstitial fluid flow. Biotechnol Bioeng. 1994; 43:573-581.

[9] Gardinier JD, Majumdar S, Duncan RL, Wang LY. Cyclic hydraulic pressure and fluid flow differentially modulate cytoskeleton re-organization in MC3T3 osteoblasts. Cell Mol Bioeng. 2009; 2:133-143.

[10] Basso N, Heersche JNM. Characteristics of in vitro osteoblastic cell loading models. Bone. 2002; 30:347-351.

[11] Freed LE, Vunjak-Novakovic G. Tissue engineering bioreactors. In: Lanza RP; Langer R, Vacanti J. editors, Principles of Tissue Engineering. San Diego, CA: Academic Press. 2000; p:143-156.

[12] Bancroft GN, Sikavitsas VI, Milos AG. Design of a flow perfusion bioreactor system for bone tissue engineering applications. Tiss Eng. 2003; 9:549-554.

[13] Kapur S, Baylink DJ, Lau KH. Fluid flow shear stress stimulates human osteoblast proliferation and differentiation through multiple interacting and competing signal transduction

bioRxiv preprint doi: https://doi.org/10.1101/146159; this version posted June 5, 2017. The copyright holder for this preprint (which was not certified by peer review) is the author/funder. All rights reserved. No reuse allowed without permission.

pathways. Bone. 2003; 32:241-251.

[14] Lee DY, Yeh CR, Chang SF, Lee PL, Chien S, Cheng CK, Chiu JJ. Integrin-mediated expression of bone formation-related genes in osteoblastlike cells in response to fluid shear stress: roles of extracellular matrix, Shc, and mitogen-activated protein kinase. J Bone Miner Res. 2008; 23:1140-1149.

[15] Chen NX, Ryder KD, Pavalko FM, Turner CH, Burr DB, Qiu J, Duncan RL. Ca2+ regulates fluid shear-induced cytoskeletal reorganization and gene expression in osteoblasts. Am J Physiol Cell Physiol. 2000;278:989-997.

[16] Liu X, Zhang X, Lee I. A quantitative study on morphological responses of osteoblastic cells to fluid shear stress. Acta Biochim. Biophys Sin. 2010;42:195–201.

[17] Horikawa A, Okada K, Sato K, Sato M. Morphological changes in osteoblastic cells (MC3T3-E1) due to fluid shear stress: cellular damage by prolonged application of fluid shear stress. Tohoku J Exp Med. 2000;191:127-137.

[18] Weinbaum S, Cowin SC, Zeng Y. A model for the excitation of osteocytes by mechanical loading-induced bone fluid shear stresses. Journal of biomechanics. 1994; 27(3): 339-360.

[19] Bancroft GN, Sikavitsas VI, Dolder J, Sheffield T, Ambrose CG, Jansen JA, Mikos AG. Fluid flow increases mineralized matrix deposition in 3D perfusion culture of marrow stromal osteoblasts in a dose-dependent manner. Proc Natl Acad Sci. 2002; 99:12600-12605.

[20] Ingber DE. Mechanosensation through integrins: cells act locally but think globally. Proc Natl Acad Sci. 2003;100:1472-1474.

[21] Myers KA, Rattner JB, Shrive NG, Hart DA. Osteoblast-like cells and fluid flow: cytoskeleton-dependent shear sensitivity. Biochem Biophys Res Commun. 2007; 364:214-219.

bioRxiv preprint doi: https://doi.org/10.1101/146159; this version posted June 5, 2017. The copyright holder for this preprint (which was not certified by peer review) is the author/funder. All rights reserved. No reuse allowed without permission.

[22] Orr AW, Helmke BP, Blackman BR, Schwartz MA. Mechanisms of mechanotransduction. Dev Cell. 2006; 10:11-20.

[23] Luo Y, Wang Y, Niu X, et al. Evaluation of the cytocompatibility of butanediamine-and RGDS-grafted poly (dl-lactic acid). European Polymer Journal. 2008; 44(5): 1390-1402.

[24] Nauman E A, Risic K J, Keaveny T M, et al. Quantitative assessment of steady and pulsatile flow fields in a parallel plate flow chamber. Annals of biomedical engineering. 1999; 27(2): 194-199.

[25] Shen XH, Yang HQ, Tang WJ, Ma D, Li M, Cheng R, Song J, Yi XF. Influence of 1 alpha，25-dihydroxy vitamin D_3 on the proliferation and differentiation of osteoblasts，and the Mrna level of Collagen I and Cbfa-1. Pract Geriatr. 2014; 28(6): 500-505.

[26] Bian Jian-chun, Gu Jian-hong, Shen Yan, Zhuo Li-ling, Wang Lin, Liu Zong-ping. Effect of 1α, 25-dihydroxy vitamin D_3 on cytoskeleton, GAP junction inter cellular communication and [Ca^{2+}] of osteoblasts. Acta Nutrimenta Sinica. 2009; 31(4): 339-343.

[27] Li Y, Wang J, Xing J, et al. Surface chemistry regulates the sensitivity and tolerability of osteoblasts to various magnitudes of fluid shear stress. Journal of Biomedical Materials Research Part A. 2016; 104(12): 2978-2991.

[28] Mikkelsen UR, Fredsted A, Gissel H, Clausen T. Excitation-induced Ca^{2+} influx and muscle damage in the rat: loss of membrane integrity and impaired force recovery. J Physiol. 2004;559:271-285.

[29] Neve A, Corrado A, Cantatore FP. Osteoblast physiology in normal and pathological conditions. Cell Tissue Res 2011;343:289-302.

[30] Giancotti FG, Ruoslahti E. Integrin signaling. Science 1999;285:1028-1032.

bioRxiv preprint doi: https://doi.org/10.1101/146159; this version posted June 5, 2017. The copyright holder for this preprint (which was not certified by peer review) is the author/funder. All rights reserved. No reuse allowed without permission.

[31] Yeatts AB, Fisher JP. Bone tissue engineering bioreactors: dynamic culture and the influence of shear stress. Bone. 2011; 48:171-181.

[32] Sikavitsas VI, Bancroft GN, Holtorf HL, Jansen JA, Mikos AG. Mineralized matrix deposition by marrow stromal osteoblasts in 3D perfusion culture increases with increasing fluid shear forces. Proc Natl Acad Sci. 2003; 100:14683-14688.

[33] Holtorf HL, Jansen JA, Mikos AG. Modulation of cell differentiation in bone tissue engineering constructs cultured in a bioreactor. Adv Exp Med Biol. 2006; 585:225-241.

[34] Kunnen S J, Leonhard W N, Semeins C, et al. Fluid shear stress-induced TGF-β/ALK5 signaling in renal epithelial cells is modulated by MEK1/2. Cellular and Molecular Life Sciences. 2017: 1-16.

[35] Collin-Osdoby P, Nickols G A, Osdoby P. Bone cell function, regulation, and communication: a role for nitric oxide. Journal of cellular biochemistry. 1995; 57(3): 399-408.

[36] Owan I, Burr D B, Turner C H, et al. Mechanotransduction in bone: osteoblasts are more responsive to fluid forces than mechanical strain. American Journal of Physiology-Cell Physiology, 1997; 273(3): C810-C815.

[37] A.D. Bakker, C. Huesa, A. Hughes, R.M. Aspden, R.J. van't Hof, J. Klein-Nulend, M. H. Helfrich. Endothelial nitric oxide synthase is not essential for nitric oxide production by osteoblasts subjected to fluid shear stress in vitro, Calcif. Tissue Int. 92 (2013) 228–239.

[38] A.D. Bakker, M. Joldersma, J. Klein-Nulend, E.H. Burger. Interactive effects of PTH and mechanical stress on nitric oxide and PGE_2 production by primary mouse osteoblastic cells. Am. J. Physiol. Endocrinol. Metab. 2003; 285:E608–E613.

[39] A.D. Bakker, K. Soejima, J. Klein-Nulend, E.H. Burger. The production of nitric oxide and

bioRxiv preprint doi: https://doi.org/10.1101/146159; this version posted June 5, 2017. The copyright holder for this preprint (which was not certified by peer review) is the author/funder. All rights reserved. No reuse allowed without permission.

prostaglandin E2 by primary bone cells is shear stress dependent, J. Biomech. 2001; 34: 671–677.

[40] H.M. Willems, E.G. Van den Heuvel, G. Carmeliet, A. Schaafsma, J. KleinNulend, A.D. Bakker. Dependent and independent effects of 1, 25-dihydroxyvitamin D_3 on nitric oxide production by osteoblasts. Steroids. 2012; 77: 126–131.

[41] Van der Meijden K, Bakker A D, van Essen H W. Mechanical loading and the synthesis of 1, 25-$(OH)_2$ D_3 in primary human osteoblasts. The Journal of steroid biochemistry and molecular biology. 2016; 156: 32-39.

[42] Hayakawa K, Tatsumi H, Sokabe M. Actin stress fibers transmit and focus force to activate mechanosensitive channels. J Cell Sci. 2008; 121(4): 496-503.

[43] Wang N, Tytell JD, Ingber DE. Mechanotransduction at a distance: mechanically coupling the extracellular matrix with the nucleus. Nature reviews Molecular cell biology. 2009; 10(1): 75-82.

[44] Shemesh T, Geiger B, Bershadsky AD. Focal adhesions as mechanosensors: a physical mechanism. Proceedings of the National Academy of Sciences of the United States of America. 2005; 102(35): 12383-12388.

[45] Young SRL, Hum J M, Rodenberg E. Non-overlapping functions for Pyk2 and FAK in osteoblasts during fluid shear stress-induced mechanotransduction. PLoS One. 2011; 6(1): e16026.

[46] Norvell SM, Ponik SM, Bowen DK, et al. Fluid shear stress induction of COX-2 protein and prostaglandin release in cultured MC3T3-E1 osteoblasts does not require intact microfilaments or microtubules. Journal of applied physiology. 2004; 96(3): 957-966.

[47] Hoshi K, Kawaki H, Takahashi I, et al. Compressive Force-Produced CCN2 Induces Osteocyte Apoptosis Through ERK1/2 Pathway. Journal of Bone and Mineral Research. 2014; 29(5): 1244-1257.

bioRxiv preprint doi: https://doi.org/10.1101/146159; this version posted June 5, 2017. The copyright holder for this preprint (which was not certified by peer review) is the author/funder. All rights reserved. No reuse allowed without permission.

[48] Pavalko FM, Chen NX, Turner CH, et al. Fluid shear-induced mechanical signaling in MC3T3-E1 osteoblasts requires cytoskeleton-integrin interactions. American Journal of Physiology-Cell Physiology. 1998; 275(6): C1591-C1601.

[49] McGarry JG, Klein-Nulend J, Prendergast PJ. The effect of cytoskeletal disruption on pulsatile fluid flow-induced nitric oxide and prostaglandin E_2 release in osteocytes and osteoblasts. Biochemical and biophysical research communications. 2005; 330(1): 341-348.

[50] Ponik SM, Pavalko FM. Formation of focal adhesions on fibronectin promotes fluid shear stress induction of COX-2 and PGE_2 release in MC3T3-E1 osteoblasts. Journal of Applied Physiology. 2004; 97(1): 135-142.